Laser power dependence of the photoluminescence from CdS_xSe_{1-x} nanoparticles in glass

2000 J. Phys.: Condens. Matter 12 1097

(http://iopscience.iop.org/0953-8984/12/6/326)

J. Phys.: Condens. Matter **12** (2000) 1097–1110. Printed in the UK PII: S0953-8984(00)06418-3

Laser power dependence of the photoluminescence from CdS_xSe_{1-x} nanoparticles in glass

Prabhat Verma†, G Irmer and J Monecke

Institute of Theoretical Physics, Freiberg University of Mining and Technology, Bernhard-von-Cotta-Strasse 4, 09596 Freiberg, Germany

Received 29 July 1999, in final form 25 November 1999

Abstract. The influence of probing laser power density on the band-edge and the trap luminescence from CdS_xSe_{1-x} nanoparticles embedded in a glass matrix is reported. Both the position and the strength of the band-edge luminescence are found to be very sensitive to the laser power. It is observed for the first time that the band-edge luminescence shifts initially towards low energy and then towards high energy with increasing laser power. The results are analysed in terms of laser-induced local heating and a band-filling mechanism, respectively, which are found to explain adequately the experimental observations. The shift due to the latter shows up only beyond a threshold value of the probing laser power density. The trap luminescence shows large contributions from surface states and undergoes photodarkening at high laser power, the degree of which depends strongly on the local temperature of the nanoparticles during illumination; this is reported here for the first time. This effect is explained in terms of a permanent trapping of charge carriers due to optical processes and thermally assisted optical processes.

1. Introduction

Filter glasses containing CdS_xSe_{1-x} nanoparticles embedded in a glass matrix have received a great deal of attention in the recent past [1–8]. Three-dimensional confinement of charge carriers into a small volume of a semiconducting nanoparticle leads to a strong modification of the electronic and optical properties of the material, if the size of the nanoparticle is comparable to the exciton Bohr radius. Semiconducting nanoparticles with diameters of a few nanometres typically contain several hundreds to several thousands of atoms, yet are too small to have bulk electronic properties. Theoretical models predict [1, 2] that the energy spectrum of such materials consists of a series of discrete lines, which change their positions with the particle size. Previous studies on size-dependent absorption spectra have suggested that the states observed in such systems are delocalized over the entire particle, and a blue-shift in the absorption edge with respect to the corresponding bulk material is observed [3, 4].

The phenomenon of quantum confinement, the presence of deep traps within the band-gap, the electron–hole and electron–phonon coupling, and the influence of the particle surface on the electronic and vibrational properties seem to play an important role in these materials, and have been the focus of many previous studies [9–15]. However, a general picture of the optical and electronic properties of these systems is still not clear. In this paper we present a systematic study of the influence of the probing laser power density on the luminescence from samples containing CdS_xSe_{1-x} nanoparticles embedded in a glass matrix, with special

† Present address: Department of Electronics and Information Science, Kyoto Institute of Technology, Kyoto 606, Japan.

0953-8984/00/061097+14$30.00

emphasis on one of the samples. Apart from the recombination at the band-gap, we have identified transitions involving deep traps associated with the surface states and the defect states. Luminescence from the deep traps shows an effect of photodarkening [5, 16–19] under strong laser illumination. Several inconsistencies in the literature concerning the relaxation dynamics of photoexcited carriers seem to be due to this photodarkening process, which is manifested in a decrease of luminescence after a strong illumination of the sample. The authors have explained this effect in terms of a permanent trapping of the carriers [17–19] and in terms of an increase in non-radiative recombinations [20]. The optical properties of the material are permanently changed in such a process; however, they can be partially restored by a heat treatment. We observed a significant decrease in the trap luminescence when our samples were subjected to a strong laser illumination for a considerable time. However, there was not much change in the band-edge luminescence. The decrease in luminescence is found to depend on the illumination time as well as on the laser power. Further, we observed for the first time that the process of photodarkening is not only related to a strong illumination of the sample, but also depends on the local temperature of the nanoparticles during illumination. This effect can be best explained in terms of the removal of radiative traps by a thermally assisted optical process at elevated local temperatures. It is generally believed [4, 19] that the fluorescence lifetime and the spectral shape for these systems depend on the pumping intensity. In this paper we show that the luminescence energy also depends on the pumping intensity. After making proper corrections for the decrease in band-gap due to local heating produced under strong illumination, we observed a net blue-shift in the band-edge luminescence with increasing pumping intensity, which is explained by the band-filling mechanism. This shift is found to be negligible up to a certain value of laser power density, beyond which the band-edge luminescence undergoes a minimum shift of 45 meV. This provides a threshold value of the power density for the band-filling process. This behaviour of the band-edge shift is reported here for the first time.

2. Experimental details

The samples investigated are orange and red sharp-cut filter glasses commercially available from Schott Glass Incorporated, Germany. Their commercial names are OG515, OG530, OG550, OG590, RG630, RG645, RG665, and RG695, where the numbers indicate the cut-off wavelengths in nanometres, and OG and RG stand for orange and red glasses, respectively. These samples are semiconductor-doped glasses and contain CdS_xSe_{1-x} nanocrystallites of dimensions of the order of nanometres, embedded in borosilicate glass matrix. The volume fraction of the nanocrystallites in the glass matrix is about 0.1%, as calculated from TEM measurements. The cut-off wavelengths for various glasses depend both on the composition x and the size of the nanocrystallites, both of which were determined by us using Raman spectroscopy [21]. A detailed study was performed on the sample OG550, which has a sulphur content of 67% ($x = 0.67$) and particle diameter of about 7.3 nm [21]. The exciting wavelength used in our experiments corresponds to an energy slightly above the band-gap of this sample.

Photoluminescence (PL) experiments were performed with the 488 nm line of an Ar-ion laser employing a triple-stage Jobin–Yvon monochromator, a liquid-nitrogen-cooled CCD or a Peltier-cooled PMT detector, and usual electronics. In the first step, in order to determine the true position and shape of luminescence bands without any influence of illumination, the experiments were performed on all samples at low probing laser power density ($\approx$10 W cm^{-2}) in a macro-chamber, where it was ensured that there were no changes in the optical properties of the samples due to laser illumination or due to laser-induced local heating. In the second step, where the temperature dependence and the effect of laser illumination on the sample

were studied, experiments were performed under a microscope, where it was possible to go up to a high power density of about 280 kW cm^{-2}. In most cases, PL spectra were recorded for a broad emission range from 490 to 900 nm. The spectral response of the CCD detector changes significantly over this range; we therefore used a PMT detector. However, in order to determine the exact position of a luminescence band, a CCD detector was also used for short emission ranges around the luminescence band. In some of the cases, where the effect of illumination was to be avoided, it was necessary to measure the position of the luminescence band during a very short detection time, and hence we also used a CCD detector for such measurements.

All PL spectra were recorded in units of cm^{-1}, which is a unit of energy, and the deconvolutions and calculations were performed in the same units. However, since the commercial names of the glass samples include cut-off wavelengths in nm (for example, OG550), it is more suitable to show PL spectra in figures in the units of wavelength (nm). Also, since it is more conventional to present band-gaps in units of eV, the calculated data in table 1 (see later) are presented in units of eV.

Temperature-dependent Raman scattering was performed in order to determine the temperature dependence of the optical phonons, which was further used to determine the laser-induced local temperature of the nanoparticles during strong-illumination PL experiments. Raman experiments were performed under the same conditions as the PL experiments. Low-temperature Raman and PL experiments were performed in a liquid-nitrogen cryostat. Unless stated otherwise, all experiments were performed on sample OG550 under a microscope at a laser power density of 200 W cm^{-2}, where there was no influence of illumination on the luminescence energy. All spectra were corrected for the instrument response.

3. Results and discussion

3.1. Band-edge and trap luminescence

Figures 1(a) and 1(b) present room temperature PL spectra for some of the samples in the OG and in the RG series, respectively, recorded at a probing power density of 10 W cm^{-2}. The composition x and the particle size are for all samples given in table 1 of reference [21]. The spectra in figure 1 are arranged in the sequence of increasing particle size. The luminescence structure indicated by the index 1 corresponds to the band-edge and can be ascribed to the band-to-band recombination and to the recombinations from states very close to the band-edge. The second structure, indicated by the index 2, which appears in the form of a broad band and changes its position between 680 to 780 nm for various samples, corresponds to the radiative recombinations associated with deep traps. An additional structure, indicated by the index 3, which appears around 860 nm for all samples, is an artifact of the spectrometer and will be ignored in the following discussion. The origin of the traps can in general be related either to surface states, or to impurity or defect states [4, 9] within the nanoparticles. The photoexcited carriers relax from the band-edge to these traps via very fast non-radiative transitions [15] before they make a radiative recombination. The two structures present in PL spectra were properly resolved using a deconvolution process in order to obtain the true values of the position, the width, and the intensity of each structure. Broken curves in figures 1(a) and 1(b) show such deconvolutions for samples OG530 and RG645, respectively, as examples.

The luminescence corresponding to the band-to-band transition is observed at the band-edge energy indicated by the manufacturer for all samples—for example, at 550 nm for the sample OG550. In many of the previous studies [4,5,9], the band-edge luminescence is reported at a shifted energy compared to the band-edge, and this fact is either ignored or not mentioned.

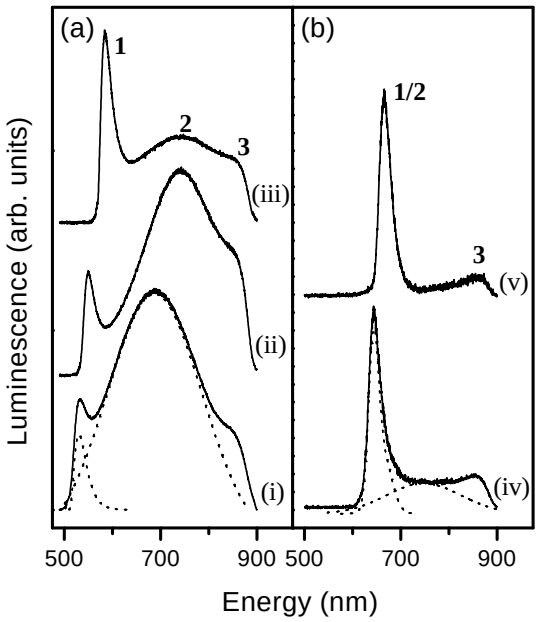

Figure 1. PL spectra from some of the samples in (a) the OG series and (b) the RG series, arranged in a sequence of increasing particle size from curves (i) to (v). The average diameters of the nanoparticles are 4.4, 7.3, 8.8, 12.0, and 15.5 nm for the samples OG530, OG550, OG590, RG645, and RG665, respectively, for curves (i) to (v). The structures indicated by indices 1 and 2 correspond to the luminescence from the recombinations at the band-edge and from the deep traps, respectively. Structure 3 is an artifact of the spectrometer. All spectra are measured at a laser power density of 10 W cm^{-2}. The broken curves in (a) and (b) represent deconvolutions for the samples OG530 and RG 645, respectively. All spectra are recorded in units of cm^{-1}, and the deconvolutions were performed on the raw data in the same units. However, in order to compare the peak positions with the commercial names of the samples, both spectra and deconvoluted curves are presented in units of nm. All spectra are presented on the same scale and are shifted vertically with respect to each other.

This observed shift is, in our opinion, due to the effects of probing laser illumination. We have found that the position of the band-edge luminescence is very sensitive to the probing laser power; this will be discussed later in this paper in more detail. As expected, the band-edge luminescence in figure 1 increases in intensity with particle size. An asymmetry on the low-energy side of structure 1 can be seen for all spectra in figure 1, which is due to the transitions from states very close to the band-edge. Our samples are extremely pure, and therefore we do not consider any impurity states close to the band-edge. It is reasonable to consider that nanoparticles do not have unwanted impurities, since they contain only a finite number of atoms and the uncontrolled impurities are normally present at a few ppm. However, there could be some defect-related states present very close to the band-edge, a mixing of which with the band-edge provides an asymmetry to the luminescence structure on the low-energy side. For measurements under high probing power densities, it is found that this asymmetry reduces considerably. The reason for this could be that the energy states above the band-edge also contribute in the recombination process for strong illumination, which gives a tail to the high-energy side of the luminescence and hence the luminescence becomes symmetric. The asymmetry in structure 1 was either ignored or was not seen in many of the previous studies; it is again, most probably, an effect of strong illumination during PL measurements.

Structure 1 in figure 1 is blue-shifted with respect to that for the corresponding bulk material due to the confinement energy. Assuming a linear variation of the band-gap with respect to the composition x in CdS_xSe_{1-x} bulk material, the band-gap of the corresponding bulk material for the sample OG550 ($x = 0.67$) should be 1.993 eV (622 nm) [22], whereas the sample OG550 shows a band-gap of 2.254 eV (550 nm). Hence the blue-shift in the band-edge luminescence in this sample due to the confinement is about 261 meV ($\approx$72 nm). When the particle size decreases, the effect of quantization on the exciton motion becomes prominent. At very small particle sizes the character of the exciton starts disappearing and the electrons and holes become individually confined [1], because the kinetic energy of the electron and hole becomes dominant and the Coulomb interaction between the electron and hole starts losing its significance. This results in a positive confinement energy, and the band-edge of the nanocrystal is blue-shifted with respect to that for the corresponding bulk material. The band-edge luminescence from the RG samples lies in the red region and has larger intensity. At the same time, the trap luminescence is weak and overlaps with the tail of the band-edge luminescence, as can be seen in figure 1(b). The structure indicated by 1/2 in figure 1(b) is dominated by the band-edge luminescence (structure 1). Structure 2, which is distinctly observed at least in the OG samples, changes remarkably in energy and intensity for various samples. Since the composition x is nearly constant [21] for the OG samples, these changes are primarily due to the variation in the particle size, which varies by about a factor of 2 from OG530 to OG590 [21]. The observed rapid decrease of the intensity of structure 2 with increasing particle size can be best explained by a significant contribution from surface states, the recombination through which is expected to be enhanced for small particles since the surface-to-volume ratio is larger. This is also the reason for the weak intensity of structure 2 in the RG samples (broken curve in figure 1(b)), because they contain larger particles. Defect-related states within the nanoparticles also contribute to this structure, but this contribution should depend only weakly on the particle size.

3.2. Photodarkening in trap luminescence

The effect of photodarkening is observed in the trap luminescence for all samples at strong laser illumination. For a detailed study of the photodarkening effect, we have investigated the sample OG550 by recording PL spectra before and after a strong laser illumination and by observing the temporal behaviour of the luminescence structures as well as of the optical phonon measured in Raman scattering experiments during illumination. The sample was shifted perpendicular to the laser beam to ensure that a fresh point was exposed in each experiment. The sample was exposed to a laser illumination of 200 kW cm^{-2} with laser energy ($\lambda = 488$ nm) slightly above the band-edge for about 40 minutes, and PL spectra were recorded before and after this illumination from the same spot. During this period, the LO-phonon position in the Raman spectra from the same spot was recorded after every five minutes. After making proper correction for the luminescence background, it was found that the Raman signal remained the same in intensity, position, and linewidth, whereas the luminescence signal for transitions involving traps decreased by a factor of more than 5. Here we would like to mention that the sample achieved a stable temperature in the first five minutes of illumination, and hence the LO phonon does not show any temperature effect during the experiment. Further, to investigate the temporal behaviour of the luminescence bands, the monochromator was set to the peak positions of the two luminescence bands, separately, and the luminescence was observed through a PMT detector as a function of time. The luminescence from the band-to-band transition remained almost unchanged, whereas the luminescence from the traps reduced very quickly in the first few minutes and saturated after about half an hour.

The fact that no changes were observed in the Raman signal under a near-resonance condition indicates that the photodarkening process does not affect the vibrational properties of the sample and that the resonant excited states are not involved in this process. The decrease of the radiative recombinations in the process of photodarkening is therefore connected only with the traps. This is also evident from a negligible change in the band-edge luminescence compared to the strong change in the trap luminescence. In a previous study [20] on glass samples, photodarkening was observed in the band-edge luminescence and it was explained in terms of an increased number of surface states, which act as non-radiative channels. In contrast, we observed no darkening effect in the band-edge luminescence, which proves that this explanation, which assumes that the number of non-radiative traps increases under illumination, is not suitable in our case. In order to understand the effect of illumination on the darkening process, PL spectra were recorded after illumination with various power densities for a long duration. It was observed that the darkening effect depends on the illumination strength and is absent at low illumination. In addition, photodarkening was found to depend strongly on the local temperature of the sample during the illumination process. There seem to have been no previous studies of photodarkening with illumination at low temperatures.

Figure 2 shows PL spectra measured from the sample OG550 before and after an illumination with a laser power density of 200 kW cm^{-2} for a duration of 40 minutes. Curves (a) and (b) in figure 2 present PL spectra after an illumination at room temperature and at liquid-nitrogen temperature, respectively, and curve (c) shows a PL spectrum from an un-illuminated spot. All spectra were recorded at room temperature with low probing power densities. Proper care was taken in recording the luminescence exactly from the pre-illuminated spot, especially when the illumination was done at low temperature. Local heating due to the laser illumination at 200 kW cm^{-2} increases the nanoparticle temperature by about 160 K (as measured by

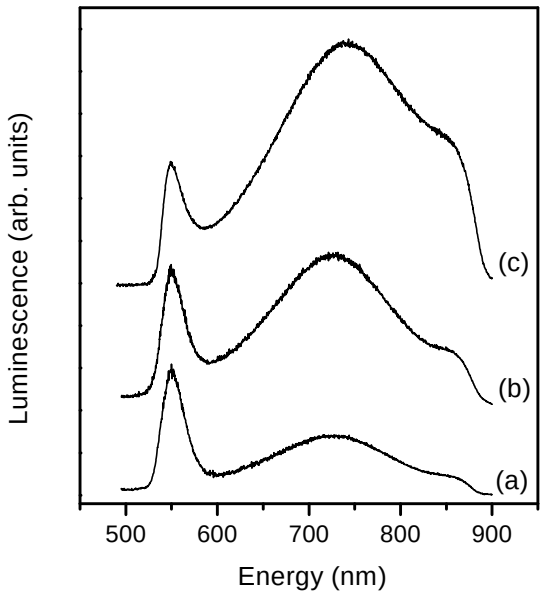

Figure 2. PL spectra from a spot on the sample OG550 which was pre-illuminated (a) at room temperature and (b) at liquid-nitrogen temperature with a laser illumination of 200 kW cm^{-2} for 40 minutes. The PL spectrum from an un-illuminated spot is shown as curve (c). After illumination, all spectra were measured at room temperature with low power density.

Raman spectroscopy; see table 1, later). Therefore, the local temperature of the sample during illumination was about 460 K and 240 K for room temperature and liquid-nitrogen temperature illuminations, respectively. It can be seen in figure 2 that the darkening effect depends strongly on the sample temperature during illumination, indicating that photodarkening is not only an optical process, but also includes thermal processes. The most probable mechanism includes a permanent trapping of photoexcited carriers in traps located within the nanoparticles by optical processes, and by thermally assisted optical processes. It was confirmed by annealing the sample at 500 K that there was no change in the luminescence due to the thermal effect alone. When the sample is illuminated at low temperature, some of the traps including surface states and defect states are permanently filled, reducing the number of available traps. In the case of the room temperature illumination, the local temperature of nanoparticles increases to 460 K. The defect- and the surface-related states are slightly modulated at this temperature, so a greater number of states trap the photoexcited carriers permanently at this temperature. This results in different darkening effects upon low- and high-temperature illuminations, as found in figure 2.

3.3. Effects of probing power density on band-edge luminescence

Figure 3 displays a sequence of PL spectra recorded from the sample OG550 at various probing power densities ranging from 10 W cm^{-2} to 280 kW cm^{-2}. An increase in the luminescence intensity with power density is observed, which is plotted for the band-edge luminescence in figure 4. The spectra in figure 3 also have an energy shift with increasing power density,

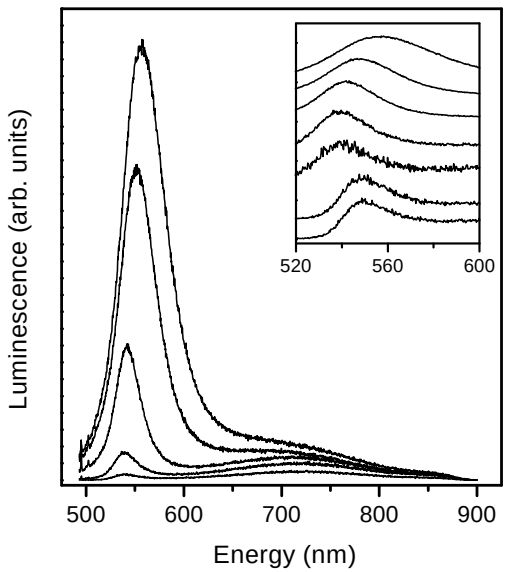

Figure 3. PL spectra recorded from the sample OG550 at probing power densities of 0.4, 4, 40, 160, and 280 kW cm^{-2} from the lower to the upper curves, respectively. The inset presents the band-edge luminescence measured at probing power densities of 0.01, 0.05, 0.4, 4, 40, 120, and 280 kW cm^{-2} from the lower to the upper curves, respectively. In order to focus attention on the position of the luminescence, the spectra in the inset are presented on a normalized scale and are shifted vertically. It can be seen from the inset that the luminescence energy is initially unchanged at 2254.2 meV (550 nm); then it shows a blue-shift to 2300.2 meV (540 nm), followed by a red-shift which goes up to 2222.7 meV (558 nm) with increasing power density.

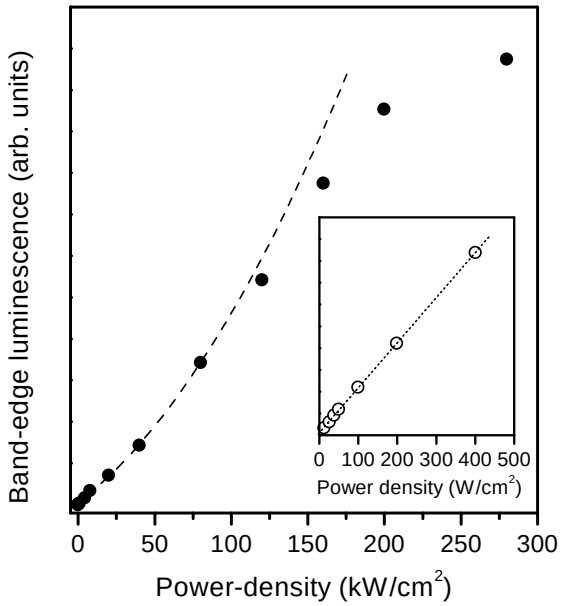

Figure 4. The probing power density dependence of the normalized band-edge luminescence efficiency for the sample OG550. Dotted curves in the inset and in the figure show that the luminescence efficiency increases linearly with laser power density up to about 400 W cm^{-2}, then it shows a parabolic dependence up to about 100 kW cm^{-2}, after which it increases slowly.

which is shown in the inset of figure 3 for the band-edge luminescence. As seen in the inset of figure 3, the band-edge luminescence does not show a uni-directional energy shift with increasing power density. The band-edge initially has a negligible shift up to a certain power density and then a large blue-shift. As the power density is further increased, a red-shift is observed, which overcomes the initial blue-shift at larger power densities. This indicates that there are two independent physical processes which give opposite shifts to the band-gap at increased probing power densities. The former process, which gives a blue-shift, starts at a threshold power density. The latter, which gives a red-shift, is weak at low power densities and becomes dominant at higher power densities. The probing laser beam is known [23] to raise the temperature of a sample. In the case of nanoparticles, the local temperature can rise considerably [24], because the particles are isolated and the heat conduction from the particles to the glass matrix is low. The band-gap of the nanoparticles therefore decreases with increasing probing power density. The red-shift in the band-edge luminescence at higher power density is due to this effect. In order to separate out the influences of the two opposite effects, it is necessary to estimate the local temperature of the nanoparticles under laser illumination and to calculate the band-gap of the nanoparticles at this temperature. This was done by performing a temperature-dependent Raman scattering study and a temperature-dependent PL study of the sample.

A mixed CdS_xSe_{1-x} crystal shows two-mode behaviour for the optical phonons in Raman spectra with two LO phonons, one corresponding to CdS and the other corresponding to CdSe. Depending upon the composition x, these phonons are shifted in energy with respect to the case for the parent materials due to the alloying effects. These phonons also suffer a small shift due to the finite size of the particles. The CdS-like phonon, which is the stronger of the two LO phonons for the sample OG550, appears at 296.7 cm^{-1} at room temperature. We

performed a temperature-dependent Raman study on this phonon at temperatures between 77 and 300 K. Due to the anharmonic effects [25–29], the optical phonons are known to show a temperature-dependent shift. In addition, the change in lattice constant with temperature modifies the vibrational potential, which provides a further shift to the LO phonon [30]. The net temperature-dependent shift in the energy of the LO phonon can therefore be given as [27–30]

$$\omega(T) = \omega_0 + C\left[1 + \frac{2}{e^{x/2} - 1}\right] + D\left[1 + \frac{3}{e^{x/3} - 1} + \frac{3}{(e^{x/3} - 1)^2}\right] + Z\omega_0 T \tag{1}$$

where $x = \hbar\omega_0/k_B T$, ω_0 is the intrinsic frequency of the LO phonon, $Z = \alpha\gamma$ with α the volume expansion coefficient and γ the Grüneisen parameter, and the parameters C and D are the anharmonic constants. The parameter Z is constant within the temperature range under consideration. The best fit to the experiments using equation (1) was obtained with $\omega_0 = 306.0\ \text{cm}^{-1}$, $C = -2.520\ \text{cm}^{-1}$, $D = -0.106\ \text{cm}^{-1}$, and $Z = 0.97 \times 10^{-5}\ \text{K}^{-1}$. With these values of the constants, equation (1) can be used to estimate the local temperature of the nanoparticles during PL measurements by measuring the energy of the LO phonon. The temperature-dependent shift of the LO phonon for the sample OG550 is shown in figure 5(a).

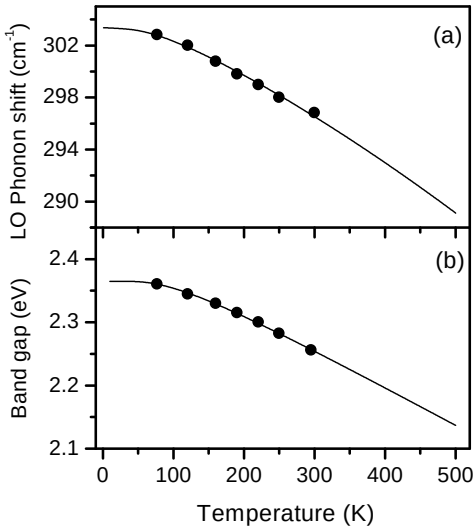

Figure 5. Temperature dependences of (a) the phonon energy for the CdS-like LO phonon in Raman spectra and (b) the band-edge luminescence energy in PL spectra for the sample OG550. The full circles represent experimental points and the curves in (a) and (b) represent theoretical fits using equations (1) and (2), respectively, which are extrapolated up to 500 K.

In order to estimate the band-gap of the nanoparticles at a particular local temperature, we measured the band-edge luminescence at various temperatures between 77 and 300 K. The band-edge luminescence at very low excitation power density corresponds to the band-gap of the sample. The temperature dependence of the band-gap of a bulk semiconductor can be given as [31–34]

$$E_g(T) = E_0 + A\left[\coth\left(\frac{B}{k_B T}\right) - 1\right] \tag{2}$$

where E_0 represents the band-gap at low temperature and A and B are temperature-independent empirical constants. This equation can be used for nanoparticles as well, assuming $E_g(T)$ and E_0 to include the confinement energy. The best fit to the experimental data using equation (2)

was obtained with $E_0 = 2364.9$ meV, $A = -86.32$ meV, and $B = 12.15$ meV and is shown in figure 5(b). Equation (2), along with these values, was used to estimate the band-gap of the nanoparticles at a given temperature.

In order to understand the behaviour of the PL spectra in figure 3, the peak position of the CdS-like LO phonon was measured in Raman scattering experiments under the same experimental conditions for each probing power density. The local temperatures and the band-gaps of the nanoparticles were estimated from equations (1) and (2), respectively. The values of the LO-phonon positions, the corresponding local temperatures, and the band-gap values at estimated temperatures for various probing power densities are listed in table 1. Since the observed band-edge luminescence shows a combination of blue- and red-shifts, one can calculate the net blue-shift by subtracting the red-shift due to the increase in local temperature from the observed luminescence energy. The net blue-shift thus calculated is listed in table 1 and is presented in figure 6 as a function of the probing power density.

Table 1. The probing laser power density dependence of the shift in the CdS-like LO phonon, the corresponding local temperature of the nanoparticles as calculated using equation (1), the band-gap at the estimated local temperature as calculated using equation (2), the observed band-edge luminescence energy, and the net blue-shift in the band-edge estimated from the difference of the observed luminescence energy and calculated band-gap energy, for the sample OG550.

Power density (kW cm^{-2})	LO phonon (cm^{-1})	T (K)	Band-gap (meV)	Luminescence (meV)	Blue-shift (meV)
0.012	296.7	300	2254.2	2254.2	0.0
0.025	296.7	300	2254.2	2254.2	0.0
0.037	296.6	300	2254.2	2254.2	0.0
0.05	296.6	300	2254.2	2254.2	0.0
0.10	296.5	300	2254.2	2254.2	0.0
0.20	296.7	300	2254.2	2254.2	0.0
0.40	296.7	300	2254.2	2299.3	45.1
0.80	296.6	300	2254.2	2300.0	45.8
4.00	296.4	305	2252.0	2300.2	48.2
8.00	296.2	310	2247.6	2298.6	51.0
20.00	295.8	322	2241.3	2295.6	54.3
40.00	295.3	336	2233.6	2291.8	58.2
80.00	294.2	367	2215.8	2280.0	64.2
120.00	293.0	400	2196.6	2266.2	69.6
160.00	291.7	433	2176.7	2251.0	74.3
200.00	290.7	461	2159.8	2238.4	78.6
280.00	289.0	500	2136.7	2222.7	86.0

3.3.1. Luminescence efficiency. The recombination dynamics of laser-generated electron–hole pairs in a confined system is complex in nature and the normal rate equations are not valid for small particles. This is because the carrier density n is no longer a continuously varying quantity. The number of free carriers N within each nanoparticle is discrete, with smallest non-zero value 1, which gives a minimum value of about 5×10^{18} cm^{-3} for n, assuming a spherical nanoparticle of diameter 7.3 nm for the sample OG550 [21]. For weak illumination, there will be a random distribution of particles with $N = 0$ and $N = 1$. With increasing laser power density the mean value of N and the number of particles with higher N will increase. The recombination in such a situation will be a rather complex competition between exciton formation and recombination, radiative recombinations at the band-gap and from traps, non-radiative recombinations, and Auger recombinations. The branching ratio could be a

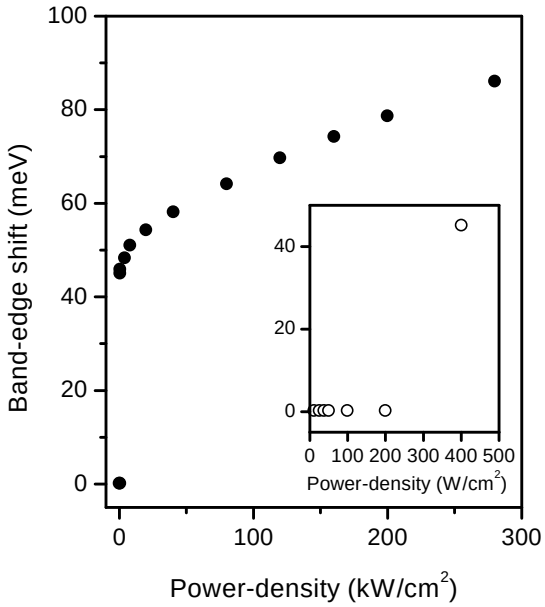

Figure 6. The dependence of the net blue-shift in the band-edge luminescence energy for the sample OG550 on the probing laser power density, after subtracting the red-shift due to laser-induced local heating. The inset shows that the shift is negligible up to 400 W cm^{-2}, after which it increases by a minimum of 45 meV.

complicated function of N, and, thus, of the probing laser power density. However, for low probing power density, where $N = 0$ or 1, the recombination is of geminate type [5, 35, 36], where the recombination dynamics is determined only by the particles with $N = 1$ and the branching ratio should be laser power independent. Owing to the confinement of carriers, a photogenerated electron in a nanoparticle with $N = 1$ can recombine only with its own hole, whereas with increasing N, there are more recombination possibilities. When $N > 1$, the recombination is non-geminate and the recombination rate is proportional to the product of the number of electrons and the number of holes, and hence includes squared terms. The luminescence is therefore expected to be a simple linear function of the laser power density at low power densities, whereas for larger values of N at higher power densities, it would include squared terms [5]. The band-edge luminescence intensity data presented in figure 4 and in the inset of figure 4 show good qualitative agreement with this argument. Luminescence intensity initially increases linearly with the probing power density up to about 400 W cm^{-2} (inset of figure 4); then it can be best fitted with a parabolic curve up to about 100 kW cm^{-2}, after which the enhancement in luminescence intensity is rather slow. At this power density, the local temperature of the nanoparticles increases by about 70 K. At higher laser power densities two important processes, namely the carrier saturation and thermal quenching [37–39], which reduce the luminescence intensity, become significant. Both effects result in a slow increase of luminescence intensity with laser power density. The charge-carrier saturation is a well known effect for bulk material, and it is expected to be more important in the case of nanoparticles, due to their finite volumes. Thermal quenching is known [38, 39] to decrease the luminescence efficiency exponentially with temperature, and, hence, it is possible that this process becomes significant when the local temperature rise in our sample becomes of the order of 200 K for maximum power density. However, we could not confirm the charge-carrier saturation

and thermal quenching processes for our experimental conditions by independent alternative methods. Similar arguments hold for the increase in the trap luminescence with laser power density; however, as seen in figure 3, there is no significant change in the trap luminescence intensity with laser power density. The reason for this could be photodarkening, because the measurement time for these experiments is about 30–40 minutes, which is enough to activate photodarkening in the trap luminescence at increased power densities.

3.3.2. Luminescence energy. The net blue-shift observed in the band-edge luminescence with increasing power density in figure 6 can be best explained in terms of the band-filling process [40–42], which is also known as the Burstein shift. The Burstein shift is not significant in a bulk material until the value of the free-carrier density n becomes large. On the other hand, since a nanoparticle has discrete energy lines compared to the continuous band for a bulk material, the band-filling becomes effective at a lower value of n for the nanoparticles compared to bulk material. This can be understood from the illustration in figure 7, which represents the schematic band-structure for a bulk and a nanostructure direct-band-gap material. In the case of a bulk material, $\vec{k}$ can take all values including zero, and hence the band-structures are parabolic, as illustrated in figure 7(a). Electrons (holes) can occupy any position on the parabolic conduction (valence) band. The band-gap is defined as the energy difference between the conduction and the valence band at $k = 0$. On the other hand, in the case of a nanoparticle, the electron wavelength is confined to the size of the particle, and hence $\vec{k}$ takes only non-zero discrete values, depending on the particle size. If k_1 represents the minimum possible value of $\vec{k}$ for a nanoparticle, then the band-gap of the nanoparticle will be E_1 (the gap at k_1, which

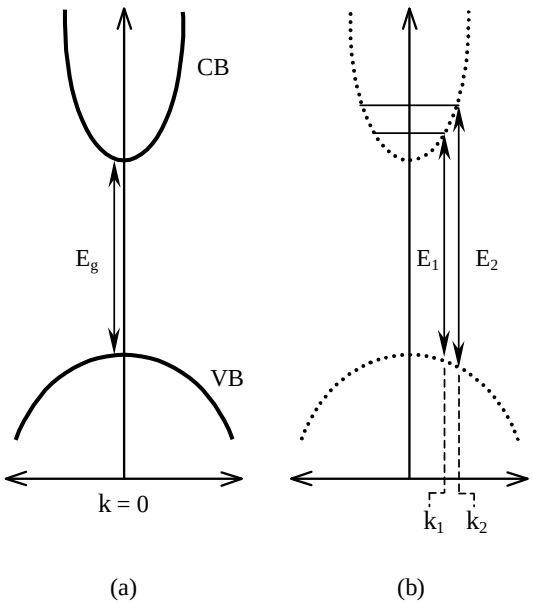

Figure 7. A schematic diagram of the electronic band-structure in (a) bulk and (b) nanoparticles. Bulk materials have parabolic bands with all possible values of $\vec{k}$ including $k = 0$. The band-gap for bulk is defined as the gap E_g at $k = 0$. On the other hand, nanoparticles have discrete values of $\vec{k}$, which gives a quantum nature to the band-structure. The band-gap is defined as the gap E_1 at k_1, the minimum possible value of $\vec{k}$. Due to the discrete positions of the electronic structures, the band-filling process is quantized and faster in nanoparticles compared to bulk.

is equal to E_g + confinement energy), as illustrated in figure 7(b). If k_2 is the next possible value of $\vec{k}$, then the electronic structure of the nanoparticle will have discrete energies E_1, E_2 and so on, as shown in figure 7(b). Therefore, at low laser power densities, where only a few electron–hole pairs are created, the bands are filled up to energy E_1. As further pairs are created at increased power density, the new pairs occupy the next possible position in the bands and the bands are filled up to E_2. Therefore, the band-filling process is much faster in nanoparticles compared to bulk, where bands are filled in a continuous manner. It can also be understood from figure 7(b) that, for nanoparticles, the bands are filled in discrete steps, providing a sudden jump in the PL energy with increasing power density. Therefore, at very low laser power density, where the average value of N for the nanoparticles is 0 or 1, there is no significant Burstein shift. As soon as N increases due to increase in the power density, the shift becomes significant. This shows an increase in the band-edge luminescence, since now recombinations involving higher energy levels also take place. As can be seen in the inset of figure 6 (also in table 1), no shift in the luminescence energy is observed up to a power density of 400 W cm^{-2}, after which a shift of 45 meV can be seen. With increasing laser power density, the luminescence shows a further shift, which goes up to 86 meV at a power density of 280 kW cm^{-2}. This indicates that most of the particles have $N = 0$ or 1 up to 400 W cm^{-2} and hence the band-filling is insignificant. As the power density is further increased, the value of N increases in some particles, which increases the band-filling by a discrete amount giving an increase of 45 meV in the peak position of the observed luminescence. The power density of 400 W cm^{-2} can be considered as the threshold value of the laser power density for invoking the Burstein shift in our sample. For higher values of N, the carrier density n can be considered to be continuous, or, in other words, the higher energy levels are very close to each other. We therefore find a continuous increase in band-edge luminescence energy for higher laser power densities in figure 6.

4. Conclusions

Filter glasses doped with semiconductor nanoparticles show two structures in photoluminescence, which are associated with the band-to-band transition at the band-edge and to the radiative transitions involving deep traps. The luminescence at the band-edge increases with the particle size, is blue-shifted due to confinement effects, and shows an asymmetry on the lower-energy side, which disappears at high laser power. The deep-trap luminescence shows large contributions from the surface states and is highly sensitive to the particle size. The transitions associated with the traps undergo photodarkening under strong laser illumination. Apart from the illumination time and intensity, the darkening effect is also influenced by the sample temperature during illumination, which shows that photodarkening is not only an optical process, but also involves thermal processes. The luminescence at the band-edge shows an increase in intensity and a shift in energy with the probing laser power density. This shift arises due to the laser-induced local heating of the nanoparticles and due to the band-filling process. The former gives rise to a red-shift and the latter, which is significant only beyond a threshold value of the laser power density, gives a blue-shift in the luminescence energy.

References

[1] Efros Al L and Efros A L 1982 *Sov. Phys.–Semicond.* B **16** 772
[2] Brus L E 1984 *J. Chem. Phys.* **80** 4403
[3] Warnock J and Awshalom D D 1985 *Phys. Rev.* B **32** 5529
[4] Zheng J P, Shi L, Choa F S, Liu P L and Kwok H S 1988 *Appl. Phys. Lett.* **53** 643

[5] Kull M and Coutaz J L 1990 *J. Opt. Soc. Am.* B **7** 1463
[6] Rodrigues P A M, Tamulaitis G, Yu P Y and Risbud S H 1995 *Solid State Commun.* **94** 583
[7] Orii T, Kaito S, Matsuishi K, Onari S and Arai T 1997 *J. Phys.: Condens. Matter* **9** 4483
[8] von Behren J, van Buuren T, Zacharias M, Chimowitz E H and Fauchet P M 1998 *Solid State Commun.* **105** 317
[9] Borrelli N F, Hall D W, Holland H J and Smith D W 1987 *J. Appl. Phys.* **61** 5399
[10] Klein M C, Hache F, Ricard D and Flytzanis C 1990 *Phys. Rev.* B **42** 11 123
[11] Inokuma T, Ricard D, Lukasik J and Flytzanis C 1990 *Phys. Rev.* B **42** 11 093
[12] Alivisatos A P, Harris T D, Carroll P J, Steigerwald M L and Brus L E 1989 *J. Chem. Phys.* **90** 3463
[13] Zheng J P and Kwok H S 1992 *J. Opt. Soc. Am.* B **9** 2047
[14] Shiang J J, Risbud S H and Alivisatos A P 1993 *J. Chem. Phys.* **98** 8432
[15] Mittleman D M, Schoenlein R W, Shiang J J, Colvin V L, Alivisatos A P and Shank C V 1994 *Phys. Rev.* B **49** 14 435
[16] Horan P and Blau W 1990 *J. Opt. Soc. Am.* B **7** 304
[17] Kull M, Coutaz J L, Manneberg G and Grivickas V 1989 *Appl. Phys. Lett* **54** 1830
[18] Malhotra J, Hagan D J and Matsuoka B G 1991 *J. Opt. Soc. Am.* B **8** 1531
[19] Roussignol P, Ricard D, Lukasik J and Flytzanis C 1987 *J. Opt. Soc. Am.* B **4** 5
[20] Němec P, Trojánek F and Malý P 1995 *Phys. Rev.* B **52** R8605
[21] Verma P, Cordts W, Irmer G and Monecke J 1999 *Phys. Rev.* B **60** 5778
[22] See, for example, Madelung O 1996 *Semiconductors—Basic Data* (Berlin: Springer) p 185
[23] Lax M 1977 *J. Appl. Phys.* **48** 3919
[24] Rodrigues P A M, Yu P Y, Tamulaitis G and Risbud S H 1996 *J. Appl. Phys.* **80** 5963
[25] Klemens P G 1966 *Phys. Rev.* **148** 845
[26] Hart T R, Aggarwal R L and Lax B 1970 *Phys. Rev.* B **1** 638
[27] Balkanski M, Wallis R F and Haro E 1983 *Phys. Rev.* B **28** 1928
[28] Verma P, Abbi S C and Jain K P 1995 *Phys. Rev.* B **51** 16 660
[29] Anand S, Verma P, Jain K P and Abbi S C 1996 *Physica* B **226** 331
[30] Irmer G, Wenzel M and Monecke J 1996 *Phys. Status Solidi* b **195** 85
[31] Viña L, Logothetidis S and Cardona M 1984 *Phys. Rev.* B **30** 1979
[32] O'Donnell K P and Chen X 1991 *Appl. Phys. Lett.* **58** 2924
[33] Pässler R 1997 *Phys. Status Solidi* b **200** 155
[34] Pässler R, Blaschta F, Griebl E, Papagelis K, Haserer B, Reisinger T, Ves S and Gebhardt W 1997 *Phys. Status Solidi* b **204** 685
[35] Street R A 1981 *Phys. Rev.* B **23** 861
[36] Roussignol P, Kull M, Ricard D, de Rougemont F, Frey R and Flytzanis C 1987 *Appl. Phys. Lett.* **51** 1882
[37] Shionoya S, Koda T, Era K and Fujiwara H 1964 *J. Phys. Soc. Japan* **19** 1157
[38] Anand S, Verma P, Abbi S C, Jain K P, Tafreshi M J, Balakrishnan K and Dhansekaran R 1996 *Pramana* **47** 133
[39] Mochizuki S and Umezawa K 1996 *J. Phys.: Condens. Matter* **8** 7509
[40] Hsu S C and Kwok H S 1987 *Appl. Phys. Lett.* **50** 1782
[41] Olbright G R, Peygambarian N, Koch S W and Banyai L 1987 *Opt. Lett.* **12** 413
[42] Burstein E 1954 *Phys. Rev.* **93** 632